NEURAL REGENERATION RESEARCH
September 2017, Volume 12, Issue 9
www.nrronline.org

RESEARCH ARTICLE

Detecting dopaminergic neuronal degeneration using diffusion tensor imaging in a rotenone-induced rat model of Parkinson's disease: fractional anisotropy and mean diffusivity values

Lan-xiang Liu[1,*], Dan Du[1], Tao Zheng[1], Yuan Fang[1], Yan-sheng Chen[1], Hui-ling Yi[1], Qing-yuan He[2], Da-wei Gao[3], Qing-lei Shi[4]
1 Department of Magnetic Resonance Imaging, First Hospital of Qinhuangdao, Qinhuangdao, Hebei Province, China
2 Department of Radiology, Peking University Third Hospital, Beijing, China
3 College of Environmental and Chemical Engineering, Yanshan University, Qinhuangdao, Hebei Province, China
4 Scientific Clinical Specialist, Siemens Ltd., Beijing, China

How to cite this article: *Liu LX, Du D, Zheng T, Fang Y, Chen YS, Yi HL, He QY, Gao DW, Shi QL (2017) Detecting dopaminergic neuronal degeneration using diffusion tensor imaging in a rotenone-induced rat model of Parkinson's disease: fractional anisotropy and mean diffusivity values. Neural Regen Res 12(9):1485-1491.*
Funding: *This work was financially supported by the Research Grant of Hebei Province Science and Technology Project of China, No. 1427777118D.*

Graphical Abstract

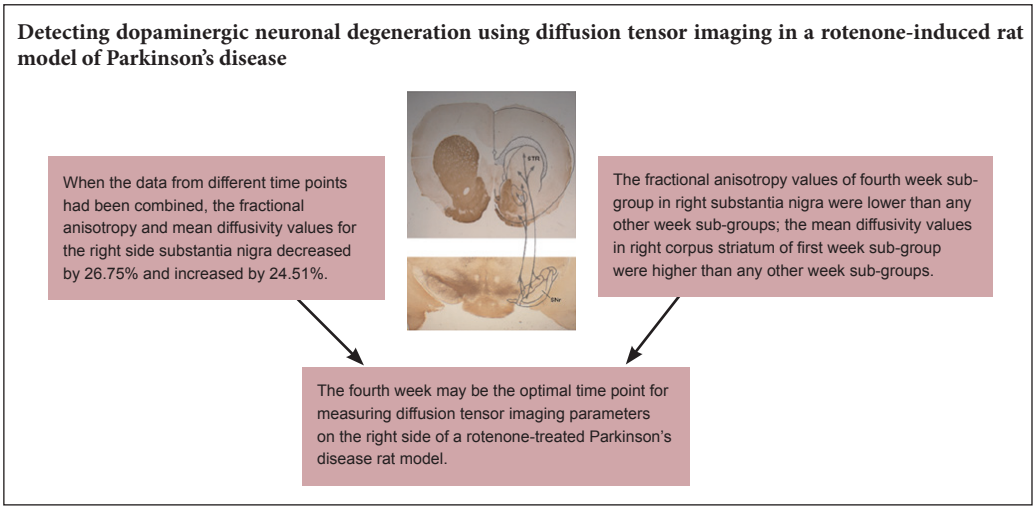

Correspondence to:
Lan-xiang Liu,
liulanxiang66@sina.com.

orcid:
0000-0002-7434-4434
(Lan-xiang Liu)

doi: *10.4103/1673-5374.213559*

Accepted: *2017-06-03*

Abstract

Dopamine content in the basal ganglia is strongly associated with the degree of dopaminergic neuron loss in the substantia nigra pars compacta. Symptoms of Parkinson's disease might not arise until more than 50% of the substantia nigra pars compacta is lost and the dopamine content in the basal ganglia is reduced by more than 80%. Greater diagnostic sensitivity and specificity would allow earlier detection of Parkinson's disease. Diffusion tensor imaging is a recently developed magnetic resonance imaging technique that measures mean diffusivity and fractional anisotropy, and responds to changes in brain microstructure. When the microscopic barrier (including cell membranes, microtubules and other structures that interfere with the free diffusion of water) is destroyed and extracellular fluid volume accumulates, the mean diffusivity value increases; when the integrity of the microstructure (such as myelin) is destroyed, fractional anisotropy value decreases. However, there is no consensus as to whether these changes can reflect the early pathological alterations in Parkinson's disease. Here, we established a rat model of Parkinson's disease by injecting rotenone (or sunflower oil in controls) into the right substantia nigra. Diffusion tensor imaging results revealed that in the stages of disease, at 1, 2, 4, and 6 weeks after rotenone injection, fractional anisotropy value decreased, but mean diffusivity values increased in the right substantia nigra in the experimental group. Fractional anisotropy values were lower at 4 weeks than at 6 weeks in the right substantia nigra of rats from the experimental group. Mean diffusivity values were markedly greater at 1 week than at 6 weeks in the right corpus striatum of rats from the experimental group. These findings suggest that mean diffusivity and fractional anisotropy values in the brain of rat models of Parkinson's disease 4 weeks after model establishment can reflect early degeneration of dopaminergic neurons. The change in fractional anisotropy values after destruction of myelin integrity is likely to be of greater early diagnostic significance than the change in mean diffusivity values.

Key Words: *nerve regeneration; diffusion tensor imaging; fractional anisotropy; mean diffusivity; magnetic resonance imaging; Parkinson's disease; rotenone; neurodegenerative disease; biomarkers; substantia nigra; tyrosine hydroxylase; neural regeneration*

Introduction

Parkinson's disease (PD) is a progressive neurodegenerative disease that is becoming increasingly prevalent in young people (Mehanna et al., 2015). Its symptoms arise late in the disease stage, and it is often difficult to distinguish from other neurodegenerative diseases (Thanawattano et al., 2015). It is important to identify PD early and begin treatment as early as possible to obtain a good prognosis (Long et al., 2012; Gazewood et al., 2013; Liang et al., 2015).

Over the past two decades, a variety of imaging techniques have been used to search for biomarkers of PD. The most common approach in magnetic resonance imaging (MRI) is voxel-based morphometry, which is used to evaluate atrophy in cortical and subcortical structures. However, voxel-based morphometry cannot be reliably used to diagnose PD (Burton et al., 2004; Ramirez-Ruiz et al., 2005; Feldmann et al., 2008; Benninger et al., 2009; Ibarretxe-Bilbao et al., 2010). Another type of imaging, proton magnetic resonance spectroscopy, demonstrated a reduction in the N-acetylaspartate/choline ratio in the lentiform nucleus of patients with PD, and an asymmetric decrease in N-acetylaspartate/creatinine ratio in the contralateral substantia nigra in patients with PD with unilateral symptoms. However, the diagnostic efficiency of this technique remains to be confirmed in further clinical experiments using strong magnetic fields (Choe et al., 1998; Clarke et al., 2000; de Celis Alonso et al., 2015). Other MRI techniques include diffusion-weighted imaging and magnetization transfer imaging; however, to date, none of these techniques have reached the accuracy and reliability required to justify their introduction into standard clinical practice or as part of interventional clinical trials. Particularly promising results have been obtained with diffusion tensor imaging (DTI) used to investigate the diffusion characteristics of the substantia nigra.

DTI can assess the random movement of protons of water molecules in terms of overall extent (mean diffusivity, MD) and orientational dependence (fractional anisotropy, FA) (Tak et al., 2016). The correlation between dopaminergic cell loss in the substantia nigra and the progressive symptoms of PD makes imaging of the substantia nigra a promising noninvasive method of examining patients with PD. Indeed, a narrowing of signals from the pars compacta of the substantia nigra was found in patients with PD (Duguid et al., 1986; Atasoy et al., 2004; Sohmiya et al., 2004). The loss of dopaminergic neurons removes diffusion barriers and their orientational dependence, which results in greater diffusivity and lower anisotropy, as demonstrated in a number of neurodegenerative diseases (Le Bihan, 1995; Abe et al., 2002; Hikishima, 2015). The DTI value has been validated for the diagnosis of PD, and negative or positive relationships between FA or MD values, as well as the degeneration of the nigrostriatal pathway, have been found (Brooks, 1995; Chesselet et al., 1996; Booij et al., 1997; Vaillancourt et al., 2009; Lewis et al., 2009; Zhan et al., 2012). Despite this, pathological data from patients in clinical trials cannot be obtained in most situations. Therefore, studying the pathogenesis, early diagnosis and treatment of PD in an established animal model remains important for obtaining pathological results.

Rotenone is a natural, fat-soluble compound extracted from *Derris elliptica*. It readily traverses cell membranes and the blood-brain barrier, without the aid of the dopamine transporter. Rotenone can specifically suppress the activity of mitochondrial complex I, which leads to the failure of oxygen utilization and energy metabolism (Friedrich et al., 1994; Qiu et al., 2016). Previous studies have reported that rotenone injected into rats can selectively damage the mesolimbic dopamine system, resulting in a successful model of PD by reproducing Lewy body development and disease progression in rats (Shiman et al., 1971; Betarbet et al., 2000; Ryu et al., 2002; Sherer et al., 2003; Tayarani-Binazir et al., 2010; Duty and Jenner, 2011; Voitenko and Nikonenko, et al., 2015). Optimal time points for such measurements have also been suggested, but are not consistent (Van Camp et al., 2009; Delli Pizzi et al., 2013).

Furthermore, decreasing neurotransmitter levels in the nigrostriatal pathway has been suggested as one of the main mechanisms of inducing PD (Tayarani-Binazir et al., 2010). Tyrosine hydroxylase (TH) is the rate-limiting enzyme in the synthesis of catecholamines and plays an important role in dopamine biosynthesis. The activity and expression of TH in striatal pathways can therefore directly affect the biosynthesis of dopamine. Therefore, variations in TH are strongly associated with the occurrence and development of PD (Valente, 2001). In patients with PD, as well as in rat models of the disease, TH shows abnormal expression and activity, from gene to enzyme (Lücking, 2000). In addition, α-synuclein, a protein discovered recently that is strongly associated with PD, is also the essential component of Lewy bodies. Although the mode of action of α-synuclein is still unclear, this protein can suppress the expression and activity of TH (Yu et al., 2004). Therefore, the level and activity of TH can be used as a biomarker for determining the success of animal models of PD.

The aims of the present study were to determine the diagnostic accuracy of DTI in a rotenone-induced rat model of PD, and to identify the optimal measurement time point using immunohistochemistry.

Materials and Methods

Animals

Thirty adult male specific-pathogen-free Sprague Dawley rats, aged 2–3 months and weighing 180–310 g, were provided by Beijing HFK Bioscience, China (animal approval No. SCXK (Jing) 2009-0004). The rats were fed a rodent chow and purified water, and were housed under standard conditions. All procedures and housing conditions followed international ethical statutes and laws for the protection of animals, and were approved by the Animal Ethics Committee of First Hospital of Qinhuangdao, China (approval No. 20140018).

PD model establishment

The rats were randomly allocated to two groups (control, n = 6; experimental, n = 24). All rats were anesthetized with an intraperitoneal injection of 0.6 mL pentobarbital (Cat. No. P8410; 0.3%; Solarbio, Beijing, China) and placed in a ste-

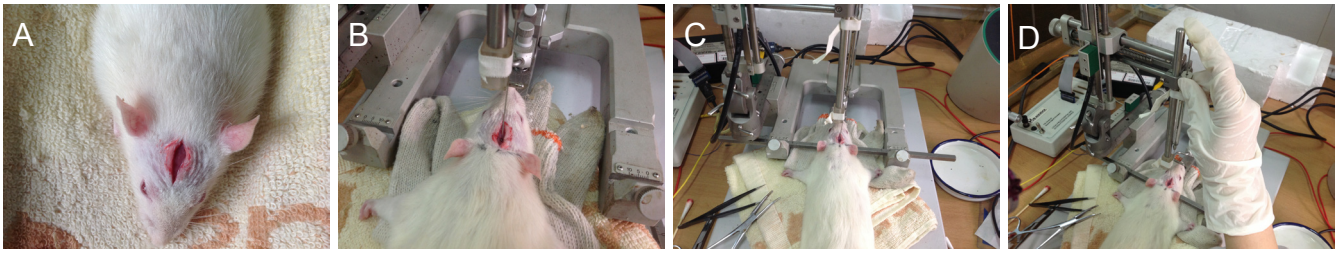

Figure 1 Parkinson's disease model establishment: rotenone injection into the substantia nigra.
(A) Skull exposure: The fur on the head was shaved and a 2–3 cm incision was made in the scalp; fascia and soft tissue were separated to reveal the skull, and the bregma was marked (8.4 mm relative to the middle of the external auditory canal). (B) Needle positioning: the needle was inserted into the right substantia nigra (anteroposterior, −4.8 mm; lateral, +1.9 mm; dorsoventral, −8.5 mm relative to bregma). (C, D) Rotenone was injected slowly (0.2 μL/min) by hand using a microsyringe, which was maintained in place for 10 minutes after injection before being withdrawn slowly.

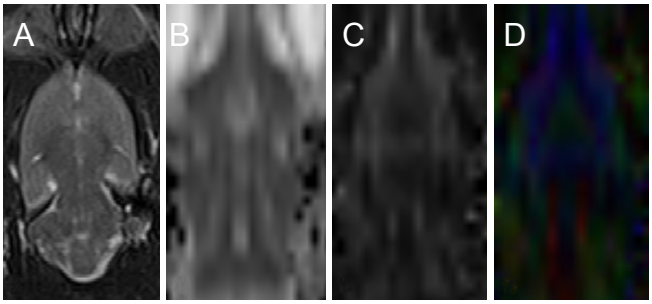

Figure 2 Coronal imaging of mouse brain.
(A) T2 weighted image; (B) mean diffusion image; (C) fractional anisotropy image; (D) color fractional anisotropy map (red, right/left direction; green, anterior/posterior direction; blue, superior/inferior direction).

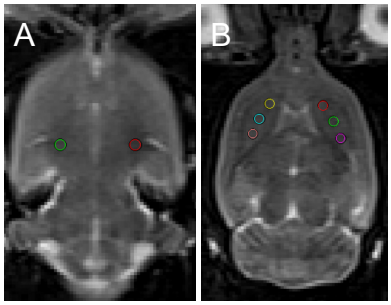

Figure 3 Coronal T2-weighted images showing selection of regions of interest.
(A) In the substantia nigra; (B) in three subdivisions of the corpus striatum (head, body, and tail).

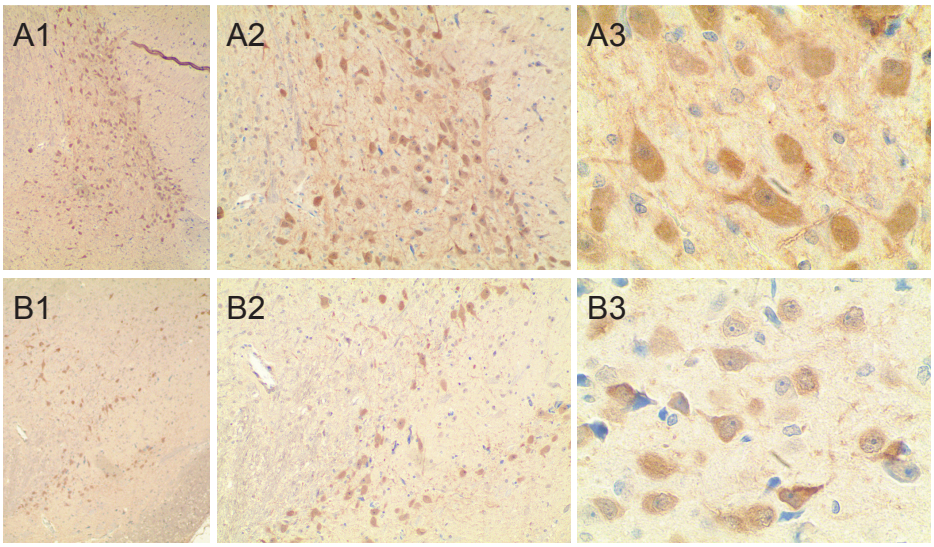

Figure 4 Tyrosine hydroxylase (TH) immunohistochemistry in the substantia nigra 6 weeks after rotenone injection (light microscopy).
Representative images of TH-immunopositive cells in the rat substantia nigra of the control group (A1–A3) and experimental group (B1–B3). Original magnification: 40× (A1, B1), 100× (A2, B2), 400× (A3, B3). Compared with the control group, the experimental group showed damaged neuronal morphology, some nuclear pyknosis, fewer TH-positive cells, and lightly stained cytoplasm.

reotaxic frame. The injection position for the right substantia nigra was determined using the following stereotaxic coordinates from bregma: anteroposterior, −4.8 mm; mediolateral, 1.9 mm; dorsoventral, −7.8 mm (**Figure 1**). Rats in the control group received an injection of 2 μL sunflower oil, and those in the experimental group received 3 μg rotenone (No. R8875-1G) dissolved in 2 μL dimethyl sulfoxide. Twelve rats died from intolerance to anesthesia or hemorrhage during injection, leaving 12 in the experimental group.

Rats in the experimental group showed rotational behavior 10 minutes after apomorphine (0.25 mg/kg intraperitoneally) was administered, 1, 2, 4, and 6 weeks after surgery (Sindhu, et al., 2005) and the number of rotations was counted within 30 minutes. A rotational speed greater than 7 rotations/minute indicated the model had been established successfully.

MR image acquisition and post-processing

At 1, 2, 4, and 6 weeks after surgery, all 18 rats were anes-

thetized with pentobarbital (0.6 mL intraperitoneally) and placed onto temperature-controlled animal beds in a 3.0 Tesla MRI scanner (Magnetom Verior; Siemens, Erlangen, Germany) with a 4-channel, 50 mm diameter phased array animal coil (part number: 10-F04885). The imaging protocol comprised coronal (cT2WI) and transverse (tT2WI) whole-brain T2-weighted imaging, and coronal (c)DTI. The cT2WI and cDTI sequences had identical slice thickness, slice gap and slice number and were located at the same level of the substantia nigra. The anatomical structures of the corpus striatum, midbrain and most of the medulla were included in cT2WI and cDTI image acquisition.

MRI parameters were as follows: cT2WI turbo spin echo (repetition time/echo time = 3,000/113 ms, flip angle = 150°, field of view = 74 mm × 74 mm, average = 14, voxel size = 0.3 mm × 0.3 mm × 2.0 mm, slice thickness = 2.0 mm, number of slices = 10); tT2WI turbo spin echo (repetition time/echo time = 4,000/111 ms, flip angle = 150°, average = 10, field of view = 70 mm × 70 mm, voxel size = 0.4 mm × 0.3 mm × 2.0 mm, slice thickness = 2.0 mm, number of slices = 12). With the same slice orientation and position as cT2WI, single-shot echo-planar imaging was used in DTI and the settings were as follows: repetition time/echo time = 1,800/110 ms, field of view = 74 mm × 74 mm, slice thickness = 2 mm, voxel size = 1.5 mm × 1.0 mm × 2.0 mm, sensitivity encoding factor = 2, nonlinear directions = 15, *b*-value = 0/1,000 s/mm^2. To increase the signal-to-noise ratio, scanning was repeated nine times (total scanning time = 17 minutes, 38 seconds).

Imaging analysis was carried out using prototype software on a workstation (Siemens Verio 3.0 T MR Leonardo 3682). MD and FA maps of mouse brains were compared with coronal T2WI slices (**Figure 2**). One radiologist with 10 years of experience in neural MRI, who was blinded to experimental grouping, placed circular regions of interest (ROI) measuring 0.30–0.60 cm^2 in the center of the substantia nigra and in the head, body, and tail sub-regions of the corpus striatum on both sides (**Figure 3**). To increase the accuracy of the measured values, freehand ROIs were carefully matched to the margins of the corpus striatum and the substantia nigra, first using cT2WI images as reference images and then copying them to corresponding parameter maps. The final values for the corpus striatum and substantia nigra were calculated from, respectively, the average values of the three sub-regions of the corpus striatum and the mean parameters of the substantia nigra.

Immunohistochemistry

After MRI at 6 weeks, rats were killed by decapitation under deep anesthesia using 0.6 mL pentobarbital (Solarbio, Beijing, China). Coronal sections (15 μm thickness) were cut using a cryostat and mounted in paraffin. Brain sections were incubated overnight at 4°C with rabbit anti-rat TH antibody (1:300; Abcam, Cambridge, UK), followed by horseradish peroxidase-conjugated goat anti-mouse IgG (SP-9001; Beijing Zhongshan Golden Bridge Biotechnology, Beijing, China) for 30 minutes at 37°C. 3,3′-Diaminobenzidine was used for visualization. Lastly, all tissue specimens were stained with hematoxylin and eosin and viewed under a light microscope (Olympus, Tokyo, Japan) equipped with a CCD camera (Leica DMI4000B, Germany). Neuronal changes (shape of TH-immunoreactive cells and the level of cytoplasm staining in the substantia nigra) were examined by a pathologist with 30 years of experience in neuropathological examination.

Statistical analysis

Statistical comparisons were performed using SPSS 16.0 software (SPSS, Chicago, IL, USA). All data are presented as the mean ± SD. A two sample *t*-test was used to test the difference in FA and MD values in the substantia nigra and corpus striatum between the control and experimental groups on both sides. Comparisons between every time point of FA and MD were analyzed using repeated measures analysis of variance and the Bonferroni test. The null hypothesis (the error covariance matrix of the orthonormalized transformed dependent variables is proportional to an identity matrix) was tested using Mauchly's test of sphericity. The Greenhouse-Geisser method was used to adjust the degrees of freedom for the average tests of significance. $P < 0.05$ was considered statistically significant.

Results

Comparison of FA and MD values between control and experimental groups after combining data at all time points

When the data from all four time points were combined, the FA value in the right substantia nigra was 26.75% ($F = 20.64$, $P < 0.001$) lower in the experimental group than in the control group, and the MD value was 24.51% ($F = 8.16$, $P = 0.01$) greater than that in the control group. There were no significant differences in FA or MD values between experimental and control groups on either side of the corpus striatum, or in the FA value in the left substantia nigra, when data from all time points were combined (**Table 1**). Repeated measures analysis of variance revealed no significant trend over time, and no interaction between time and group for the FA and MD values in either region ($P > 0.05$).

FA and MD values for the substantia nigra and corpus striatum on both sides in the experimental group

In the experimental group, FA values in the right substantia nigra were lower at 4 weeks than at 1, 2, and 6 weeks, with a significant difference between 4 and 6 weeks. MD values in the right corpus striatum were higher at 1 week than 2, 4 and 6 weeks, with a significant difference between 1 and 6 weeks ($P < 0.05$; **Table 2**). No significant differences were found for FA and MD values on the left side of the substantia nigra or corpus striatum.

Comparisons of the FA and MD values between the control and experimental groups at each time point

Right substantia nigra FA values were significantly lower in the experimental group than in the control group at different time points. MD values in the experimental group were sig-

Table 2 Comparison of fractional anisotropy and mean diffusivity values between control and experimental groups at 1–6 weeks after model establishment

	1 week		2 weeks		4 weeks		6 weeks	
	Control	Experimental	Control	Experimental	Control	Experimental	Control	Experimental
Fractional anisotropy								
Right substantia nigra	0.231±0.008	0.171±0.047*	0.232±0.013	0.176±0.037*	0.229±0.020	0.142±0.015*#	0.220±0.020	0.178±0.029*
Left substantia nigra	0.229±0.021	0.239±0.037	0.226±0.014	0.230±0.042	0.229±0.022	0.239±0.041	0.230±0.011	0.253±0.033
Right corpus striatum	0.127±0.025	0.120±0.016	0.116±0.010	0.122±0.020	0.117±0.009	0.127±0.016	0.127±0.015	0.117±0.014
Left corpus striatum	0.126±0.025	0.123±0.017	0.122±0.014	0.126±0.016	0.121±0.008	0.128±0.013	0.124±0.017	0.135±0.024
Mean diffusion ($\times 10^{-3}$ mm^2/s)								
Right substantia nigra	0.718±0.089	1.009±0.308*	0.724±0.057	0.879±0.274	0.740±0.049	0.810±0.198	0.719±0.084	0.918±0.313
Left substantia nigra	0.661±0.058	0.752±0.099	0.654±0.047	0.675±0.102	0.681±0.082	0.733±0.081	0.690±0.058	0.709±0.073
Right corpus striatum	0.743±0.052	0.728±0.046#	0.709±0.055	0.732±0.064	0.675±0.050	0.690±0.068	0.663±0.044	0.679±0.037
Left corpus striatum	0.751±0.067	0.728±0.069	0.718±0.058	0.720±0.062	0.676±0.059	0.717±0.045	0.686±0.023	0.713±0.052

*P < 0.05, *vs.* control group; #P < 0.05, *vs.* 6 weeks after model establishment (mean ± SD; n = 6 rats in control group, n = 12 rats in experimental group; repeated measures analysis of variance and Bonferroni test). Control rats received 2 μL sunflower oil; experimental rats received 3 μg rotenone to establish a model of Parkinson's disease.

Table 1 Fractional anisotropy and mean diffusivity values derived from DTI between control and experimental groups (combined time points)

	Control group	Experimental group
Fractional anisotropy		
Right substantia nigra	0.228±0.016	0.167±0.036**
Left substantia nigra	0.229±0.016	0.240±0.038
Right corpus striatum	0.122±0.016	0.121±0.027
Left corpus striatum	0.126±0.017	0.118±0.026
Mean diffusion ($\times 10^{-3}$ mm^2/s)		
Right substantia nigra	0.726±0.068	0.904±0.278*
Left substantia nigra	0.671±0.061	0.717±0.091
Right corpus striatum	0.697±0.057	0.707±0.078
Left corpus striatum	0.708±0.059	0.719±0.115

*P < 0.05, **P < 0.01, *vs.* control group (mean ± SD; n = 6 rats in control group; n = 12 rats in experimental group; two sample t-test). Control rats were injected with 2 μL sunflower oil; experimental rats were injected with 3 μg rotenone to establish a model of Parkinson's disease.

nificantly higher than in the control group in the first subgroup (P < 0.05; **Table 2**).

Immunohistochemistry results

The right substantia nigra of the experimental group showed changes in neuronal morphology and nuclear condensation. In addition, there were fewer TH-immunopositive cells, and the cytoplasm was less strongly stained, in the experimental group than in the control group. There were no notable observations on the left side or in the control group (**Figure 4**).

Discussion

MRI can provide important information *in vivo*, allowing the examination of cortical or subcortical regions in patients with PD. However, conventional MRI techniques can only provide limited information for diagnosis and therapeutic monitoring, and are mainly used to discriminate PD from atypical syndromes, exclude secondary features such as vascular lesions, and confirm the absence of specific imaging features found in atypical parkinsonism. High-field DTI has been reported to detect regional and specific alterations in the microscopic integrity of the white matter and basal ganglia known to be involved in PD pathology (Baglieri et al., 2013). Significant correlations between the alteration of DTI-derived parameters in the putamen, and other regions affected in PD, were also found in the context of PD subtypes. Therefore, microstructural alterations detected with high field DTI could be used as biomarkers for the diagnosis and monitoring of PD (Zhan et al., 2012).

Here, we evaluated the feasibility of using FA and MD values for diagnosing PD in rotenone-induced rat models, and examined the corresponding morphological characteristics. When the data from all time points were combined, lower FA values and higher MD values were observed in the right substantia nigra in the experimental group than in the left substantia nigra or control group. The reason for this may be a degeneration of dopaminergic neurons and an increase in water content in the PD models. Additionally, after multivariate analysis of FA values in the right substantia nigra, significant differences were detected between the control and experimental groups at various time points, whereas for MD values only the first week showed a significant difference between groups. This suggests that FA values are a more sensitive measure of dopaminergic neuronal degeneration than MD values. Moreover, FA values in the right substantia nigra in the experimental group were lower at 4 weeks than at 1, 2, and 6 weeks, with a significant difference between 4 and 6 weeks. The reason for this may be that degeneration of dopaminergic neurons is more advanced, suggesting that this is the optimal time point at which to measure effects in rotenone-induced PD rat models on the experimental side.

These findings were in agreement with the literature investigating the role of DTI-derived parameters in PD rat models. For example, Boska et al. (2007) reported that the MD value increased and the FA value decreased in the substantia nigra in rats 5–7 days after PD model establishment using

1-methyl-4-phenyl-1,2,3,6-tetrahydropyridine, and this was validated using histochemistry. Furthermore, Boska's study demonstrated that the FA value in the right substantia nigra was lowest at 4 weeks, but increased at 6 weeks, nearly reaching the original level. The reason for this may be gliosis and inflammation of the nuclei, or intrusion of surrounding fibers into the shrinking structure (Rosas et al., 2006; Guo et al., 2015; Lenfeldt et al., 2015). It might also be due to a decrease in anisotropy of the molecular microstructure in the early stages (1–4 weeks) that was restored at a later stage (6 weeks). Similarly, other than the changes in water diffusion in the right substantia nigra, the changes in MD in weeks 1–6 in the right substantia nigra in the experimental group might also be caused by the same factors. Changes in MD value, a DTI-derived parameter, in the right corpus striatum and other anatomical structures indicated secondary damage, which may have been caused *via* the cortico-striato-nigral pathway. This pathway comprises fiber connections between the substantia nigra, corpus striatum and putamen, as confirmed by neuroanatomy and pathology (Blackwell et al., 2003).

However, our results differ from those reported by Van Camp et al. (2009), in which FA values in the ipsilateral substantia nigra were elevated. This might be due to differences in protocol between the present study and theirs. First, in their experiment, 6-hydroxydopamine was used to produce the model. This would cause the production of free radicals, which would attack the cell membrane and lead to over-oxidation. Secondly, the injection volume in their experiment was 4 μL, whereas we used 2 μL. This difference may have affected the degeneration of the nigrostriatal pathway (Przedborski et al., 1995; Ferro et al., 2005; Kondoh et al., 2005). Third, the anatomical structure into which they injected 6-hydroxydopamine was the corpus striatum, whereas we injected our rats in the substantia nigra. All these factors may have caused the differences between Van Camp et al.'s experiment and ours.

Histologically, we observed fewer TH-immunopositive cells and less cytoplasmic staining in our experimental animals than in the control animals, and pyknosis occurred. These changes indicate the destruction of dopaminergic neurons in the substantia nigra, confirming our model was established successfully. Therefore, it seems that the FA and MD values reflect the neuronal damage in the PD model, suggesting they are promising biomarkers in the diagnosis and therapeutic monitoring of the disease.

Our study has some limitations. First, the sample size was small; future studies with large samples should be conducted to determine the reproducibility of the results. Second, due to limited experimental conditions, the substantia nigra could not be measured separately. Third, all ROIs were determined manually for the DTI, which might have given rise to measurement error in the FA and MD calculations. However, as MRI and post-processing techniques are developed, DTI will certainly play an increasingly important role in the diagnosis and monitoring of PD.

In summary, the DTI-derived parameters FA and MD provide valuable information for the detection of dopaminergic neuron damage in a rotenone-induced rat model of PD. The FA value seems to be more sensitive to dopaminergic neuron damage than the MD value. In addition, our results suggest that 4 weeks after rotenone administration may be the optimal time point for measuring DTI parameters in rat models.

Acknowledgments: *We thank Dr. Hong-bin Han from Beijing Key Laboratory of Magnetic Resonance Imaging Device and Technique for his generous technical help. We would like to thank Dr. Min Zhao and Fang Xiao from Department of Pathology, First Hospital of Qinhuangdao for their technical instructions in immunohistochemistry.*

Author contributions: *LXL, YF, DD, and QYH designed this study. DD and TZ performed experiments. DD, YSC, HLY, and QLS analyzed data. DD and DWG wrote the paper. All authors approved the final version of the paper.*

Conflicts of interest: *None declared.*

Research ethics: *The study protocol was approved by the Animal Ethics Committee of First Hospital of Qinhuangdao (approval No. 20140018). The experimental procedure followed the United States National Institutes of Health Guide for the Care and Use of Laboratory Animals (NIH Publication No. 85-23, revised 1986).*

Data sharing statement: *The datasets analyzed during the current study are available from the corresponding author on reasonable request.*

Plagiarism check: *Checked twice by iThenticate.*

Peer review: *Externally peer reviewed.*

References

Abe O, Aoki S, Hayashi N, Yamada H, Kunimatsu A, Mori H, Yoshikawa, T, Okubo, T, Ohtomo K (2002) Normal aging in the central nervous system: quantitative MR diffusion-tensor analysis. Neurobiol Aging 23:433-441.

Atasoy HT, Nuyan O, Tunc T, Yorubulut M, Unal AE, Inan LE (2004) T2-weighted MRI in Parkinson's disease; substantia nigra pars compacta hypointensity correlates with the clinical scores. Neurol India 52:332-337.

Baglieri A. Marino MA, Morabito R, Di LorenzoG, Bramanti P, Marino S (2013) Differences between conventional and nonconventional MRI techniques in Parkinson's disease. Funct Neurol 28:73-82.

Benninger DH, Thees S, Kollias SS, Bassetti CL, Waldvogel D (2009) Morphological differences in Parkinson's disease with and without rest tremor. J Neurol 256:256-263.

Betarbet R, Sherer TB, MacKenzie G, Garcia-Osuna M, Panov AV, Greenamyre JT (2000) Chronic systemic pesticide exposure reproduces features of Parkinson's disease. Nat Neurosci 3:1301-1306.

Blackwell KT, Czubayko U, Plenz D (2003) Quantitative estimate of synaptic inputs to striatal neurons during up and down states in vitro. J Neurosci 23:9123-9132.

Booij J, Tissingh G, Boer GJ, Speelman JD, Stoof JC, Janssen AG, Wolters EC, van Royen EA (1997) [^{123}I]FP-CIT SPECT shows a pronounced decline of striatal dopamine transporter labelling in early and advanced Parkinson's disease. J Neurol Neurosurg Psychiatry 62:133-140.

Boska MD (2007) Quantitative diffusion tensor imaging detects dopaminergic neuronal degeneration in a murine model of Parkinson's disease. Neurobiol Dis 26:590-596.

Brooks DJ (1995) The role of the basal ganglia in motor control: contributions from PET. J Neurol Sci 128:1-13.

Burton EJ, McKeith IG, Burn DJ, Williams ED, O'Brien JT (2004) Cerebral atrophy in Parkinson's disease with and without dementia: a comparison with Alzheimer's disease, dementia with Lewy bodies and controls. Brain 127:791-800.

Chesselet MF, Delfs JM (1996) Basal ganglia and movement disorders: an update. Trends Neurosci 19:417-422.

Choe BY, Park JW, Lee KS, Son BC, Kim MC, Kim BS, Suh TS, Lee HK, Shinn KS (1998) Neuronal laterality in Parkinson's disease with unilateral symptom by in vivo ^{1}H magnetic resonance spectroscopy. Invest Radiol 33:450-455.

Clarke CE, Lowry M (2000) Basal ganglia metabolite concentrations in idiopathic Parkinson's disease and multiple system atrophy measured by proton magnetic resonance spectroscopy. Eur J Neurol 7:661-665.

de Celis Alonso B, Hidalgo-Tobón SS, Menéndez-González M, Salas-Pacheco J, Arias-Carrión O (2015) Magnetic resonance techniques applied to the diagnosis and treatment of parkinson's disease. Front Neurol 6:146.

Delli Pizzi S, Rossi C, Di Matteo V, Esposito E, Guarnieri S, Mariggio MA, Franciotti R, Caulo M, Thomas A, Onofrj M, Tartaro A, Bonanni L (2013) Morphological and metabolic changes in the nigro-striatal pathway of synthetic proteasome inhibitor (PSI)-treated rats: a MRI and MRS study. PLoS One 8:e56501.

Duguid JR, De La Paz R, DeGroot J (1986) Magnetic resonance imaging of the midbrain in Parkinson's disease. Ann Neurol 20:744-747.

Duty S, Jenner P (2011) Animal models of Parkinson's disease: a source of novel treatments and clues to the cause of the disease. Br J Pharmacol 164:1357-1391.

Feldmann A, Illes Z, Kosztolanyi P, Illes E, Mike A, Kover F, Balas I, Kovacs N, Nagy F, (2008) Morphometric changes of gray matter in Parkinson's disease with depression: a voxel-based morphometry study. Mov Disord 23:42-46.

Ferro MM, Bellissimo MI, Anselmo-Franci JA, Angellucci ME, Canteras NS, Da Cunha C (2005) Comparison of bilaterally 6-OHDA- and MPTP-lesioned rats as models of the early phase of Parkinson's disease: histological, neurochemical and memory alterations. Neurosci Methods 148:78-87.

Friedrich T, Ohnishi T, Forche E, Kunze B, Jansen R, Trowitzsch W, Hofle G, Reichenbach H, Weiss H (1994) Two binding sites for naturally occurring inhibitors in mitochondrial and bacterial NADH: ubiquinone oxidoreductase (complex I). Biochem Soc Trans 22:226-230.

Gazewood JD, Richards DR, Clebak K (2013) Parkinson disease: an update. Am Fam Physician 87:267-273.

Guo Y, Duan WR, Ma C, Jiang CQ, Xie YK, Hao HW (2015) Biocompatibility and magnetic resonance imaging characteristics of carbon nanotube yarn neural electrodes in a rat model. Biomed Eng Online 14:118.

Hikishima K (2015) Parkinson disease: diffusion MR imaging to detect nigrostriatal pathway loss in a marmoset model treated with 1-Methyl-4-phenyl-1, 2, 3, 6-tetrahydropyridine. Radiology 275:430-437.

Ibarretxe-Bilbao N, Ramirez-Ruiz B, Junque C, Marti MJ, Valldeoriola F, Bargallo N, Juanes S, Tolosa E (2010) Differential progression of brain atrophy in Parkinson disease with and without visual hallucinations. J Neurol Neurosurg Psychiatry 81:650-657.

Kondoh T, Bannai M, Nishino H, Torii K (2005) 6-Hydroxydopamine-induced lesions in a rat model of hemi-Parkinson's disease monitored by magnetic resonance imaging. Exp Neurol 192:194-202.

Le Bihan D (1995) Molecular diffusion, tissue microdynamics and microstructure. NMR Biomed 8:375-386.

Lenfeldt N, Larsson A, Nyberg L, Birgander R, Forsgren L (2015) Fractional anisotropy in the substantia nigra in Parkinson's disease: a complex picture. Eur J Neurol 22:1408-1414.

Lewis SJ, Barker RA (2009) Understanding the dopaminergic deficits in Parkinson's disease: insights into disease heterogeneity. J Clin Neurosci 16:620-625.

Liang XM, Fu GH, Zhang BC (2015) Effects of midbrain neural stem cells and bone marrow stromal stem cells on behaviors and brain morphology of rats with Parkinson's disease. Zhongguo Zuzhi Gongcheng Yanjiu 20:5838-5842.

Long D, Wang J, Xuan M, Gu Q, Xu X, Kong D, Zhang M (2012) Automatic classification of early Parkinson's disease with multi-Modal MR imaging. PLoS One 7:e47714.

Lücking CB (2000) Association between Early-onset Parkinson's Disease and Mutations in the Parkin Gene. N Engl J Med 342:1560-1567.

Mehanna R, Moore S, Hou JG, Sarwar AI, Lai E, Mehanna R (2014) Comparing clinical features of young onset, middle onset and late onset Parkinson's disease. Parkinsonism Relat Disord 20:530-534.

Przedborski S, Levivier M, Jiang H, Ferreira M, Jackson-Lewis V, Donaldson D, Togasaki DM (1995) Dose-dependent lesions of the dopaminergic nigrostriatal pathway induced by intrastriatal injection of 6-hydroxydopamine. Neuroscience 67:631-647.

Qiu S, Li JG, Qiu Q, Chen H, Xiang ZM (2016) Caffeic acid phenethyl ester against cellular injuries in the rotenone-induced Parkinson's disease model. Zhongguo Zuzhi Gongcheng Yanjiu 20:5979-5985.

Ramirez-Ruiz B, Marti MJ, Tolosa E, Bartres-Faz D, Summerfield C, Salgado-Pineda P, Gomez-Anson B, Junque C (2005) Longitudinal evaluation of cerebral morphological changes in Parkinson's disease with and without dementia. J Neurol 252:1345-1352.

Rosas HD, Tuch DS, Hevelone ND, Zaleta AK, Vangel M, Hersch SM, Salat DH (2006) Diffusion tensor imaging in presymptomatic and early huntington's disease: selective white matter pathology and its relationship to clinical measures. Mov Disord 21:1317-1325.

Ryu EJ, Harding HP, Angelastro JM, Vitolo OV, Ron D, Greene LA (2002) Endoplasmic reticulum stress and the unfolded protein response in cellular models of Parkinson's disease. J Neurosci 22:10690-10698.

Sherer TB, Kim JH, Betarbet R, Greenamyre JT (2003) Subcutaneous rotenone exposure causes highly selective dopaminergic degeneration and alphasynuclein aggregation. Exp Neurol 179:9-16.

Shiman R, Akino M (1971) Solubilization and partial purification of tyrosine hydroxylase from bovine adrenal medulla. J Biol Chem 246:1330-1334.

Sindhu KM, Saravanan KS, Mohanakumar KP (2005) Behavioral differences in a rotenone-induced hemiparkinsonian rat model developed following intranigral or median forebrain bundle infusion. Brain Res 1051:25-34.

Sohmiya M, Tanaka M, Aihara Y, Okamoto K (2004) Structural changes in the midbrain with aging and Parkinson's disease: an MRI study. Neurobiol Aging 25:449-453.

Tak HJ, Kim JH, Son SM (2016) Developmental process of the arcuate fasciculus from infancy to adolescence: a diffusion tensor imaging study. Neural Regen Res 11:937-943.

Tayarani-Binazir K, Jackson MJ, Rose S, McCreary AC, Jenner P (2010) The partial dopamine agonist pardoprunox (SLV308) administered in combination with l-dopa improves efficacy and decreases dyskinesia in MPTP treated common marmosets. Exp Neurol 226:320-327.

Thanawattano C, Pongthornseri R, Anan C, Dumnin S, Bhidayasiri R (2015) Temporal fluctuations of tremor signals from inertial sensor: a preliminary study in differentiating Parkinson's disease from essential tremor. Biomed Eng Online 14:101.

Vaillancourt DE, Spraker MB, Prodoeh J, Abraham I, Corcos DM, Zhou XJ, Comella C L, Little DM (2009) High-resolution diffusion tensor imaging in the substantia nigra of de novo Parkinson disease. Neurology 72:1378-1384.

Valente EM, Bentivoglio AR, Dixon PH, Ferraris A, Ialongo T, Frontali M, Albanese A, Wood NW (2001) Localization of a novel locus for autosomal recessive early-onset Parkinsonism, PARK6, on chromosome 1p35-36. Am Hum Genet 68:895-900.

Van Camp N, Blockx I, Verhoye M, Casteels C, Coun F, Leemans A, Sijbers J, Baekelandt V, Van Laere K, Van der Linden A (2009) Diffusion tensor imaging in a rat model of Parkinson's disease after lesioning of the nigrostriatal tract. NMR Biomed 22:697-706.

Voitenko LP, Nikonenko AG (2015) Modification of experimental rotenone model of Parkinson's disease. Fiziol Zh 61:83-90.

Yu S, Zuo X, Li Y, Zhang C, Zhou M, Zhang YA, Uéda K, Chan P (2004) Inhibition of tyrosine hydroxylase expression in α-synulein transfected dopaminergic neuronal cells. Neurosci Lett 367:34-39.

Zhan W, Kang GA, Glass GA, Zhang Y, Shirley C, Millin R, Possin KL, Nezamzadeh M, Weiner MW, Marks WJ Jr, Schuff N (2012) Regional alterations of brain microstructure in Parkinson's disease using diffusion tensor imaging. Mov Disord 27:90-97.

Copyedited by Slone-Murphy J, Maxwell R, Wang J, Li CH, Qiu Y, Song LP, Zhao M